Int. J. Electron. Commun. (AEÜ) 65 (2011) 901–905

Contents lists available at ScienceDirect

International Journal of Electronics and Communications (AEÜ)

journal homepage: www.elsevier.de/aeue

Hilbert-shaped complementary single split ring resonator and low-pass filter with ultra-wide stopband, excellent selectivity and low insertion-loss

He-Xiu Xu[a,*], Guang-Ming Wang[a], Chen-Xin Zhang[a], Qing Peng[b]

[a] *Radar Engineering Department, Missile Institute of Air Force Engineering University, Sanyuan County 713800, China*
[b] *School of Foreign Language, Nanchang University, Nanchang 330031, China*

ARTICLE INFO

Article history:
Received 15 May 2010
Accepted 25 February 2011

Keywords:
Fractal
Multi-band
Ultra-wide stop-band
Complementary single split ring resonator (CSSRR)
Low pass filter (LPF)
Steep rejection
Negative permittivity

ABSTRACT

A novel Hilbert-shaped complementary single split ring resonator (H-CSSRR) with an alterative split gap was initially presented and studied. Transmission characteristics of several CSSRR cells were assessed by full-wave electromagnetic (EM) simulation and analyzed by electrical simulation (equivalent circuit model). Miniaturization mechanism as well as effective EM parameters retrieval is also involved. Comparing to conventional CSSRR, proposed H-CSSRR was demonstrated with a merit of lower primary transmission zero realized by negative effective permittivity and multi-resonance behavior attributing to self-similarity of Hilbert geometry. For application, a tunable assembled low-pass filter (LPF) by periodically loading H-CSSRR cells and open stubs is designed, fabricated and measured. Measurement results indicate that the designed LPF has many good performances such as relative low insertion loss (maximum 0.59 dB) in passband, ultra-wide stop-band characterized by 20 dB insertion loss (from 2.45 to 25 GHz) as well as steep rejection with sharp transition band (2.15–2.45 GHz) out of band. Excellent property and consistent numerical and experimental results of the developed LPF have confirmed the effectiveness of this design concept.

1. Introduction

Microwave low pass filters (LPF) are important and widely used to suppress harmonics and spurious signals. Recently, LPF with miniaturized dimensions, ultra-wide stopband, minimum insertion loss and enhanced selectivity is highly desirable and a challenging constraint in modern wireless communication systems. To meet these requirements, extensive experimental works and several techniques have been reported in previous literatures, e.g., LPFs implemented by defected ground structure (DGS) [1–3] as well as complementary split ring resonators (CSRRs) [4,5], employing electromagnetic band gap (EBG) [6–8], utilizing line section and an interdigital capacitor [9], stepped-impedance hairpin resonators [10], and even two-section elliptic-function LPF based on distributed elements [11].

Although covered LPFs achieved good performances in some fields of above-mentioned performances, few or even none of them met the requirement of comprehensive behavior. Some of them are also with significant drawbacks which should be emphasized in following aspects, such as insufficient stopband bandwidth, large transition band, and deteriorative return loss. On the other hand, it has been fully demonstrated that microstrip line loaded with CSRRs exhibits stopband behavior [4]. In view of them, we proposed a novel LPF from a markedly different perspective in this work.

The paper is well organized as follows. In Section 2, a microstrip resonator element with tunable lower transmission zero based on Hilbert-shaped complementary single split ring resonator (H-CSSRR) is presented and studied in depth. For further validation, an effective electromagnetic (EM) parameters retrieval method is developed. Fractal perturbation in CSSRR is from the point of view of miniaturization and multi-band suppression. Then based on this, in Section 3, an assembled ultra-wide stopband LPF is developed by periodically cascading proposed H-CSSRR cells and open stubs. Finally, a major conclusion is presented in Section 4.

2. Proposed H-CSSRR cell

2.1. Configuration and equivalent circuit model

Classical Hilbert curve is particularly interesting due to its strong capability of space-filling and multi-band behavior. As outlined in Fig. 1, it consists of a continuous line which connects the centers of a uniform background grid. Suppose the curve filled in a square section of S as external side. By increasing the iteration level, the

---

* Corresponding author.
E-mail address: hxxu20008@yahoo.cn (H.-X. Xu).

1434-8411/$ – see front matter © 2011 Elsevier GmbH. All rights reserved.
doi:10.1016/j.aeue.2011.02.012

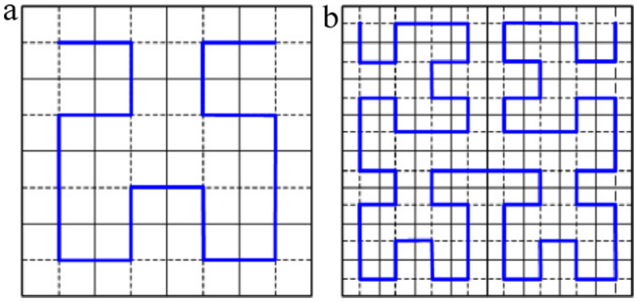

Fig. 1. Hilbert curves of (a) first ($n = 1$) and (b) second ($n = 2$) iteration level, respectively. For case $n = 2$, the Hausdorff dimension is $\ln 63/\ln 8 \approx 2$.

space between lines diminishes accordingly and the length of total perimeter increases as

$$L(n) = (2^n + 1)S \tag{1}$$

For end-coupled microstrip resonators in this paper, conventional Hilbert curves are not convenient for current application since it features two open ends on the opposite sides. In virtue of it, a simple transformation of conventional Hilbert curve should be performed to form a close loop. Fig. 2 plots the configuration of the proposed H-CSSRR as well as its equivalent circuit model. As can be observed from Fig. 2(a), H-CSSRR cell is composed of an alterative split gap in the changed closed-loop Hilbert curve which is constructed by extending the start and the end point of the second-order Hilbert curve by length of the minimum fractal segment, and then joining the terminals together with an additional line segment. The confined second iteration of the fractals is a tradeoff between miniaturization and coupling effect of neighboring segment which in turn affects the performance of LPF. Note that additional difference of H-CSSRR to conventional CSSRR is the alterative position of split gap. With the purpose of providing a deep insight into the operation mechanism of fractals and influence of changed location of split gap, the improved CSSRR (I-CSSRR) cell with alterative split gap and conventional CSSRR are also provided for comparison. Physical parameters of these CSSRR cells are kept identical except the fractal perturbation and alterative position of the split gap.

In the equivalent circuit model, outlined in Fig. 2(b), whereas L represents the line inductance, L_s models the asymmetry influence resulting from the alterative split gap, C consists of the line capacitance and the electric coupling between conductor line and CSSRR which is described by means of a resonant tank formed by parallel capacitance C_p and the inductance L_p. When it comes to conventional CSSRR cell, L_s should be removed or set to be zero. Thus the circuit model of conventional CSSRR can be considered as a special case of I-CSSRR or H-CSSRR.

2.2. Transmission characteristics and effective EM parameters

In order to verify the correctness of the presented circuit model and clarify the transmission characteristics of H-CSSRR cell. Additional study has been implemented by employing EM simulation through planar EM simulator *Ansoft Designer* and electrical parameters extraction method (electrical simulation) through *Ansoft Serenade*. During the extraction process, we have applied the equivalent T-circuit model in *Serenade* to determine the electrical lumped parameters by matching the S-parameters of the circuit model to the EM simulated ones. The substrate used in the whole design and experiment for LPF is the RT/duroid 5880 with a dielectric constant $\varepsilon_r = 2.2$ and a thickness of $h = 0.78$ mm. An H-CSSRR and an I-CSSRR cell example with physical parameters identical with the largest element in Table 2 were simulated.

Figs. 3 and 4 display the S-parameters of H-CSSRR and I-CSSRR cell, respectively. Reasonable agreement between EM and electrical simulation can be observed in the plotted frequency band. The slight discrepancy of S-parameters magnitude between them is attributing to the lossless case considered in the circuit model. By comparing S-parameters between H-CSSRR and I-CSSRR cell, we conclude that a clear lower transmission zero 2.63 GHz (approximately reduced by 42.2% compared with 4.55 GHz for I-CSSRR case)

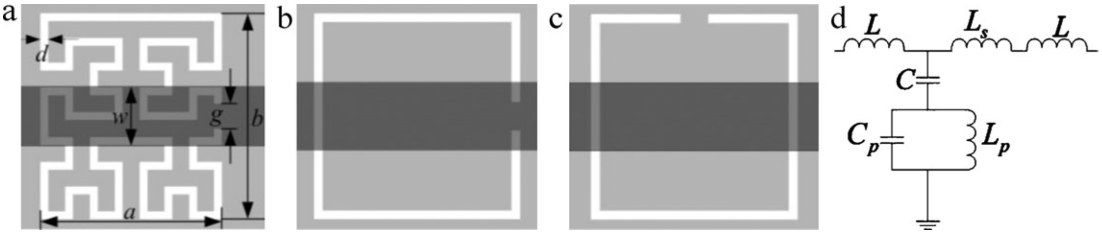

Fig. 2. Geometry of the CSSRR cells (a) H-CSSRR cell with alterative split gap in the center of left or right side of Hilbert curve, (b) I-CSSRR cell with alterative split gap in the center of left or right side of rectangle loop, (c) conventional one with split gap in the center of top or bottom side of rectangle loop, and (d) correlative equivalent T-circuit model. Whereas the CSSRR, ground plane and conductor line are depicted in white, light grey and dark grey, respectively. Note that microstrip line is located above the center of the resultant CSSRR.

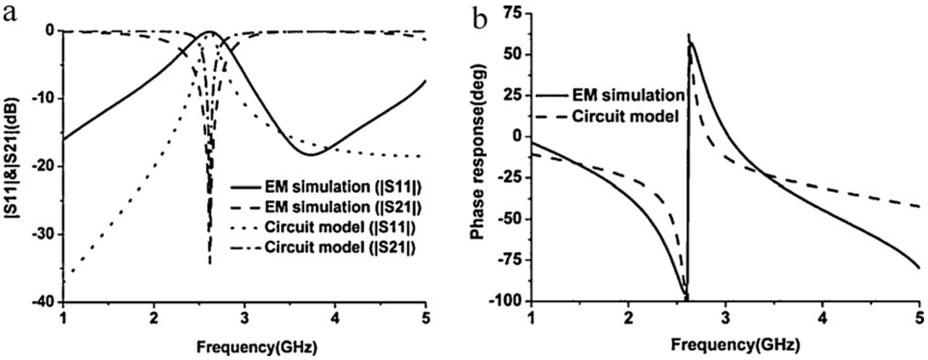

Fig. 3. S-parameters of H-CSSRR cell (a) return and insertion loss and (b) transmission phase response.